A rapid compression expansion machine (RCEM) for measuring species histories

M. Werler, R. Schießl, U. Maas
Karlsruhe Institute of Technologie
Karlsruhe, Germany

1 Introduction

Ignition delay time (IDT) is an important quantity for characterizing the auto-ignition behaviour of a fuel. A frequent use of IDT measurements is for the validation of reaction mechanisms [1–3]. While correct prediction of IDTs is a necessary requirement for a valid reaction mechanism, it is not necessarily sufficient. For a more extensive validation, additional quantities of characterisation, i.e., flame speeds or species formation have to be considered [2, 4–6]. Most measurements of temporal species profiles are conducted in flow reactors or shock tubes. For instance, Davidson et al. measured time resolved multiple species by laser absorption in their shock tube [7]. In flow reactors, species time profiles can be measured by probe sampling using, for example gas chromatography [8] or Fourier transform infrared spectrometer [9].

To access an additional range of conditions for species measurements, rapid compression machines (RCM) can be very useful. Minetti et al. [10] reported species measurements during the ignition delay period of n-heptane. They rapidly quench the reacting mixture by bursting a diaphragm, allowing the gas to expand into a collection vessel, and subsequently analyse the sample by gas chromatography and mass spectroscopy (GC/MS) [10]. Karwat et al. [11] compared species time profiles of n-heptane air mixtures in their rapid compression facility with predictions of a reaction mechanism. They used a fast valve to take probes of the test gas and analyzed it by GC/MS, demonstrating the benefit of an additional reaction mechanism validation by means of temporal profiles of intermediate species and products [11].

In the present study, another method for measuring species profiles in RCMs is introduced. Based on an existing RCM, a rapid compression/expansion machine (RCEM) was developed, which allows quenching of chemical reactions by a quick retraction of the RCMs piston at some predefined time after compression (hold time).

In this paper, first the setup of the RCEM is outlined. An efficient numerical model for describing the RCEM process and the involved heat loss is introduced and its outcome compared to CFD-simulations. To characterize the process, pressure histories resulting from multiple compression/expansion sequences are discussed. First examples of quasi-time resolved species measurements conducted with the RCEM are presented.

Correspondence to: robert.schiessl@kit.edu

2 Experimental Setup

The RCEM test rig is an extension of the RCM facility explained in Werler et al. [12]. In the following, only a description of the modifications of the setup and the new expansion mechanism are explained in detail. Figure 1 sketches the RCEM and its working principle. The combustion chamber is equipped with a creviced shaped piston, similar to other RCM's [13–15]. It is embedded in an oilbath to ensure a well-defined initial temperature. The time-resolved in-cylinder pressure is determined by a combination of an absolute pressure gauge (MKS Baratron 121A) and a quartz pressure transducer (Kistler 6061B). To record the transient piston position, a potentiometric position sensor (Burster type 7812) is connected to the driving rod. The driving

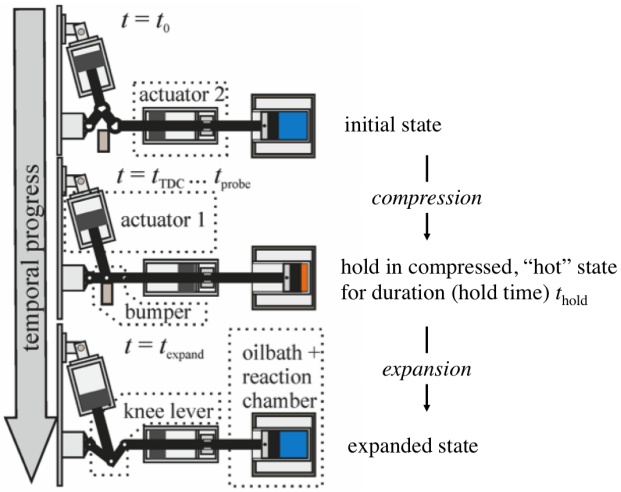

Figure 1: Scheme of the RCEM's working principle: Compression, hold in compressed state for duration (hold time) t_{hold}, expand. Gas sampling after expansion.

unit consists of pneumatic actuators and a knee-lever (cf. Figure 1). Two pneumatic actuators are connected to the driving rod, one horizontally and another one almost vertically on the hinge of the knee-lever. The use of buffer air tanks keeps the force of the actuators during compression nearly constant. When the actuators are fully pressurized, a pneumatic clamp prevents the driving rod from moving. By releasing the clamp, the experiment and the data acquisition start. For compression, the vertical actuator is employed, optionally supported by the horizontal actuator for investigations at high pressures. When the piston reaches top dead center, the knee-lever hits the bumper in its elongated position. By this, the piston is stopped immediately and locked in its top dead center position. After a pre-defined duration of this compressed state (hold time t_{hold}), the bumper can optionally be removed using another pneumatic actuator (for simplicity, not shown in Figure 1) connected to the bumper. Then, the still pressurized vertical actuator pushes the knee-lever down. This quickly pulls the piston outwards, resulting in an expansion of the gas in the combustion chamber (Figure 1).

The expansion in the RCEM quickly lowers the in-cylinder gas pressure and temperature, thereby largely freezing the ongoing chemical reactions involving stable species. This allows a subsequent, convenient probe sampling and ex-situ gas analysis, without requiring high-speed measurement devices. Note that the gas composition may change during expansion, e.g., due to the fast recombination of radicals. However, simulations considering the expansion time with the model explained below didn't show a big influence of

this recombination reactions on the composition of the detectable stable species.

To measure species time profiles, several RCEM compression/expansion cycles with identical initial conditions and compression processes can be performed. The duration between compression and expansion (hold time t_{hold}), can be varied between different experiments to achieve a species time profile. By delivering the sample to an optically accessible tube, the absorption spectra of the test gas can be analysed to detect formaldehyde. The measurement system features a deuterium light source (Ocean Optics D2000), which supplies continuous radiation in the region from 200 to 450 nm, and a UV-VIS spectrograph (Ocean Optics USB4000). A more detailed analysis of the test gas is possible with a micro gas chromatograph (Agilent 490 Micro GC). The micro GC is equipped with 3 chromatography columns, namely MS5A, PPU and a 5CB. Among the detectable species are permanent gases and hydrocarbons up to C_{10}.

3 Simulation concept

Various numerical models are commonly used to describe and compare RCM measurements to simulations. A common approach for modeling ignition processes in RCMs is the one described by Mittal et al. [13]. The temporal volume of an assumed adiabatic core (AC) in the RCM is calculated from a pressure trace of a non-reactive measurement. This accounts for the compression phase and the effect of the post-compression heat loss on the adiabatic core. However, it describes the adiabatic core only, not the whole combustion chamber.

For the newly developed measurement concept for species compositions in the RCEM, a model for the whole combustion chamber is used, namely a multi-zone homogeneous reactor model. Here, the reaction chamber is notionally subdivided into multiple disjoint zones, which are arranged in an onion-like fashion (Figure 2). Within one zone, all scalar fields are assumed to be spatially uniform, but both composition and temperature can differ from zone to zone. The zones have the same instantaneous (but temporally variable) pressure and they are closed for mass flows. As a further constraint, the sum of all zone volumes has to match the known total volume of the combustion chamber. Adjacent zones can exchange heat and each zone can do work by changing its volume. The heat exchanged between two zones or the outermost zone and the wall is calculated from their temporally varying contact surface, a heat transfer coefficient and the temperature difference.

Figure 2: Scheme of the multi-zone model

Two different heat transfer coefficients are considered, namely one for inter-zone heat transfer and one for heat transfer between the outermost zone and wall. The two heat transfer coefficients are calibrated by non-reactive RCEM experiments via fitting the pressure profile predicted by the multi-zone model to the experimental pressure profile. This procedure follows the idea of the AC model [13]. The multi-zone model can treat a time-dependent cylinder volume; it can therefore include also the compression- and expansion-phase of the RCEM, including chemical reactions which may commence or be terminated during these phases [2]. This allows modeling a quenching of chemical reactions, as it occurs in the RCEM.

4 Validation of the MZ-model

To validate the multi-zone model, it is compared to a CFD-simulation of the compression and post-compression period in the RCEM combustion chamber filled with pure nitrogen. Due to a lack of possibility to validate the CFD-simulation, it was executed according to the descriptions of Mittal et al., who found a good agreement by comparing their simulation to experimentally determined temperature distributions using PLIF in a similar combustion chamber geometry [16, 17]. The simulation was conducted for a two-dimensional configuration with rotational symmetry using a structured grid. Several CFD-runs with incressingly refined grids were performed until a grid-independent solution was achieved.

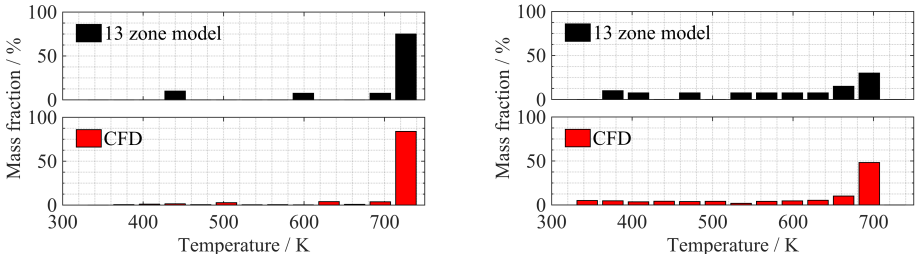

Figure 3: Comparison of temperature histograms at $t = t_{\mathrm{TDC}} + 25\,\mathrm{ms}$ (left) and $t = t_{\mathrm{TDC}} + 170\,\mathrm{ms}$ (right).

Temperature histograms from the CFD-simulation and from the multi-zone model with 13 zones are compared in figure 3. The left diagrams are for 25 ms post compression. Both the multi-zone model and the CFD simulation show that the majority of the mass in the chamber at the highest temperature. Both models also exhibit a thin thermal boundary layer, which is slightly more dispersed over the whole temperature range for the CFD-simulation. This is to be expected due to the much higher resolution of the CFD compared to the multi-zone model.

At a time of 170 ms after compression (right diagrams in fig. 3), the effect of the heat losses can be seen. The mass with a high temperature decreased, while the mass with a low temperature increased. The histograms are very similar for both simulations. The maximum temperatures and the spread of the temperature histograms agree well between both simulations. The higher resolution of the CFD-model leads to a slightly higher mass fraction in the highest temperature interval. In summary, we conclude that the MZ-model is able to describe the boundary layer and colder areas of the combustion chamber, despite its simplicity compared to the CFD-simulation. Furthermore, it is able to describe the kinetically very important high temperature in the combustion chamber center satisfactorily.

In the left diagram of Figure 4, the temperature during and after inert gas compression as predicted by the AC-model is compared to the temperature of the inner most zone of the MZ-model. As outlined above, both models used an experimental volume trace as input. The slight wiggle of the curves immedately after the end of compression reflects a spurious post-compression piston oscillation in the experiment. AC- and MZ-model agree well for at least 120 ms after compression; after this, heat transfer from the center to the adjacent zone takes place in the MZ-model. The long-term non-adiabatic behaviour can not be captured by the AC-model. For standard RCM-operation, where relevant time scales mostly do not exceed 100 ms, this is uncritical. However, for the RCEM with its longer associated time scales (up to several hundred ms), the MZ model with fidelity also for longer time spans is required.

A comparison of multiple RCEM-measurements with expansion at different times after compression (hold times) is shown in the right diagram of Figure 4. A fuel-rich mixture of CH_4/DME(90/10 mol-%) with air

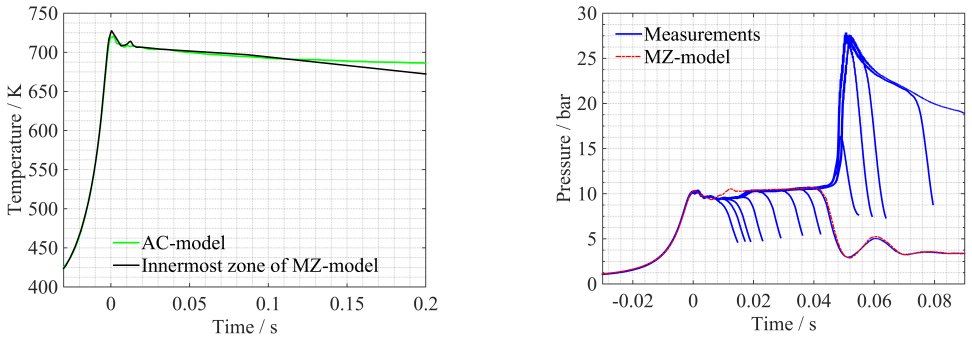

Figure 4: Left diagram: Comparison of the core temperature of the MZ- model vs. AC-model. Right diagram: Repeatability of RCEM measurements and description of the expansion process.

was investigated. For all measurements, the temperature at TDC was 727 K $\pm$ 1.8 K and the pressure was 10.2 bar $\pm$90 mbar. The good shot-to-shot repeatability enables quasi time-resolved species measurements via probe sampling from shots with different hold times. The exemplary comparison of a pressure trace from the MZ-model to a measurement shows its ability to also describe the expansion process.

5 Comparison of experimental and numerical results

A comparison between RCEM species measurements and MZ-model simulations is presented to show the potential for validating chemical kinetic mechanisms by comparing the species evolutions over time. For these sample comparisons, a newly developed mechanism by Porras et al. [18] was applied.

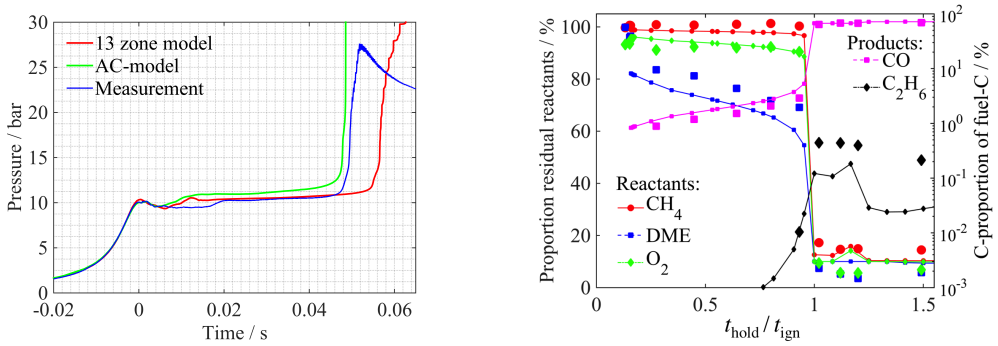

Figure 5: Investigated mixture: Fuel (90 mol% CH_4 and 10 mol% DME) in air at $\phi = 2$, $p_{OT} = 10.2$ bar and $T_{OT} = 727$ K. Left diagram: Pressure trace of measured ignition delay time compared to simulations with the AC- and the MZ-model. Right diagram: Comparison of temporal profiles of reactants and exemplary products. Measurement: big ymbols; Simulation: lines with small symbols.

A comparison between the pressure traces in the left diagram of Figure 5 shows that the heat release due to first stage ignition starts at the same time as in the AC-model. However, there is a difference in the magnitude of the pressure rise. The description of the whole combustion chamber including the crevice volume and the colder thermal boundary layer allows the hot zones, in which heat release takes place, to expand. Hence, the pressure from the MZ model fits the measurement due to the fact that the MZ-model

doesn't restrict the hot core by a volume constraint. The lower pressure increase due to first stage ignition then leads to a prolonged main ignition event.

The temporal evolution of some species (simulation and RCEM-experiments) is shown in the right diagram of fig. 5. The remaining reactant (CH_4, DME and O_2) fraction (residual reactants) and the fraction of fuel C-atoms (C-proportion of fuel-C) bound in CO and C_2H_6 are plotted. Despite the fact that the mechanism predicts the ignition delay time well, a slight discrepancy in the species evolution can be observed. The simulations show a higher consumption of fuel, while the consumption of oxygen is predicted quite well. The higher consumption of fuel also seems to lead to a higher production of CO during the ignition delay time. The production of C_2H_6 shortly before ignition is well captured by the numerical simulation. After ignition, a good agreement is observed by comparing the residual reactants and CO; the predicted amount of ethane is slightly too high, though.

To summarize, this work highlights the capability of the RCEM as an instrument for extended validation and development of reaction mechanisms by delivering species histories during reaction under well-defined conditions. The operation principle of the RCEM, as well as a numerical approach to describe the RCEM reaction process are described. In further studies, the experiment and the MZ-model will be used to improve the used mechanism under engine relevant conditions for polygeneration processes, where, beside work and heat, the formation of chemically relevant species is also in the focus.

6 Acknowledgement

Funding by the DFG as part of the research unit FOR1993 "Multifunctional conversion of chemical species and energy" within subprojects SCHI 647/3-1 and SCHI 647/3-2 is gratefully acknowledged.

References

[1] D.F. Davidson, D.F. Gauthier, R.K. Hanson, Proc. Comb. Inst. 30:1 (2005) 1175-1182.
[2] C.J. Sung, H.J. Curran, Progress in Energy and Combustion Science 44 (2014) 1-18
[3] F. Buda, R. Bounaceur, V. Warth, et al., Combust. Flame 142 (2005) 170-186.
[4] X. He, S. M. Walton, B. T. Zigler, M. S. Wooldridge, A. Atreya, Int. J. Chem. Kinet. 39 (2007) 498-517.
[5] J. de Vries, W.B. Lowry, Z. Serinyel, H.J. Curran, E.L. Petersen, Fuel 90 (2011) 331-338.
[6] Z. Chen, X. Qin, Y. Ju, Z. Zhao, M. Chaos, F.L. Dryer, Proc. Comb. Inst. 31 (2007) 1215-1222.
[7] D.F. Davidson, Z. Hong, G.L. Pilla, et al., Proc. Comb. Inst. 33 (2011) 151-157.
[8] H. Oshibe, H. Nakamura, T. Tezuka, S. Hasegawa, K. Maruta, Combust. Flame 157 (2010) 1572-1580.
[9] Z. Zhao, M. Chaos, A. Kazakov, F.L. Dryer, Int. J. Chem. Kinet., 40.1 (2008) 1-18.
[10] R. Minetti, M. Carlier, M. Ribaucour, et al., Combust. Flame 102.3 (1995) 298-309.
[11] D.M.A. Karwat, S.W. Wagnon, M.S. Wooldridge, et al., Combust. Flame 160 (2013) 2693-2706.
[12] M. Werler, L.R. Cancino, R. Schiessl, et al., Proc. Comb. Inst., 35 (2015) 259-266.
[13] G. Mittal, C.J. Sung, Combust. Sci. and Tech., 179 (2007) 497-530.
[14] J. Würmel, J.M. Simmie, Combust. Flame, 141.4 (2005) 417-430.
[15] L. Daeyup, S. Hochgreb, Combust. Flame, 114.3 (1998) 531-545.
[16] G. Mittal, M.P. Raju, und C.-J. Sung, Fuel, 94 (2012) 409-417.
[17] G. Mittal, M.P. Raju, und C.-J. Sung. Combust. Flame, 157 (2010) 1316-1324.
[18] S. Porras, R. Schießl, U. Maas. Publication in progress, 8th European Combustion Meeting (2017).